Supplemental Information (SI) Appendix for *Reconstitution of a Mycobacterium tuberculosis Proteostasis Network Highlights Essential Cofactor Interactions with Chaperone DnaK*

Tania Lupoli,[1] Allison Fay,[2] Carolina Adura,[3] Michael S. Glickman[2,4] & Carl Nathan[1]

[1]Department of Microbiology and Immunology, Weill Cornell Medicine, New York, NY-10021.

[2]Immunology Program, Memorial Sloan-Kettering Cancer Center, New York, NY-10065.

[3]High-Throughput Screening and Spectroscopy Resource Center, The Rockefeller University, New York, NY-10065.

[4]Division of Infectious Diseases, Memorial Sloan-Kettering Cancer Center, New York, NY-10065

Supplemental Method

MIC determination

Overnight log phase cultures of each strain, *mc²155*, MGM6069, MGM6160, MGM6161, and MGM6272, were diluted back to an OD600 0.005 in LBsmeg without tween-80. A 2-fold dilution series for each antibiotic was generated in a 96-well plate containing 2x the final antibiotic concentration in LBsmeg without tween-80. 100 μl of diluted culture was added to each well to generate a final dilution series from 20 μg/ml to 0.3125 μg/ml for both kanamycin and isoniazid (INH). Each strain was setup in triplicate and plates were incubated at 37°C. Pellicle formation was assessed at 72 hours.

Figure Legends

Figure S1. SDS-PAGE analysis of recombinant Mtb protein chaperones and accessory proteins. (a) Mtb DnaK, DnaJ1, DnaJ2, GrpE, and ClpB were purified from *E. coli* as N-terminal His-SUMO fusions prior to cleavage of the solubility tag. (b) Mtb Hsp20 was purified from *E. coli* with an N-terminal His-tag. For all figures, K = DnaK, J1 = DnaJ1, J2 = DnaJ2, E = GrpE, B = ClpB.

Figure S2. Standard curve of extracted ion counts (EIC) for indicated concentrations of (a) ATP and (b) ADP in quenched reaction buffers (see Methods) analyzed by Agilent Rapid Fire mass spectrometry. Error bars represent SD for n = 3.

Figure S3. Mass-spectrometry analysis of the ATPase activity of DnaK in the presence of varying [cofactor] and [substrate] shows that addition DnaJ2 and GrpE result in optimal ATP hydrolysis. (a) Example of time courses used to calculate initial rates of DnaK plus GrpE with increasing [DnaJ2] (**Figure 2c**), which is shown as relative to [DnaK]. (b) Analysis of DnaK with sub-stoichiometric DnaJ1 with varying [DnaJ2] shows that DnaJ1 does not enhance stimulation of DnaK with increasing [DnaJ2]. (c) Analysis of DnaK alone and in the presence of sub-stoichiometric DnaJ2 and GrpE with varying [DnaJ1] shows that DnaJ1 stimulates DnaK's ATPase activity at equimolar concentration in the presence or absence of other cofactors. (d) Analysis of DnaK alone and in the presence of sub-stoichiometric DnaJ1 and DnaJ2 with varying [GrpE] shows that optimal ATPase activity occurs with DnaJ2 and sub-stoichiometric GrpE. This observation agrees with the data shown in Figure 2c. A control was done with DnaJ2 and GrpE

alone (pink) to verify that the two cofactors do not possess background ATPase activity. (e) Kinetic parameters of DnaK with and without DnaJ2+GrpE. Error bars indicate SEM for n = 2.

Figure S4. Partial alignment of N-terminal protein sequences of J-proteins from Mtb (MYCTU), *M. smegmatis* (Msm) (MYCS2), *E. coli*, *S. cerevisiae* (yeast), and humans with conserved HPD motif in red. Alignment performed by Clustal Omega, where asterisks indicate identical amino acids and dots indicate similar amino acids.

Figure S5. Mass-spectrometry analysis of DnaK ATPase activity over time with wild-type J-proteins compared to point mutants in the HPD motif. (a) Initial rate analysis with sub-stoichiometric DnaJ2 wild-type, H32Q or D34E mutants plus GrpE shows that only wild-type DnaJ2 stimulates DnaK's activity. (b) Reaction analysis as described in part a except with wild-type DnaJ1 or H38Q plus GrpE illustrates that the DnaJ1 mutant is not capable of stimulating the ATPase activity of DnaK. Error bars indicate SEM for n = 2.

Figure S6. DnaJ2 and HPD point mutant H32Q co-elute with His-DnaK bound to Ni-NTA beads. (a) SDS-PAGE analysis of purified protein pull-down as described in Figure 3a except His-DnaK was not added to input. Only a faint band representing DnaJ2 can be seen in the elution (E) lane, which is enhanced in the presence of His-K. (b) Protein band quantification of replicate Figure 3a experiments. SDS-PAGE analysis using the same protocol shows that His-K co-elutes with (c) DnaJ2 and (d) DnaJ2(H32Q) in the absence of other cofactors or ClpB. (e) SDS-PAGE analysis of purified protein pull-down as described in Figure 3a except denatured luciferase plus Hsp20 (25 and 100 nM, respectively) in Buffer H was added to proteins during the incubation step. (f) Protein quantification of replicate experiments from part e. For each gel, in represents input and W represents wash steps. Band quantification performed using Image J, error bars represent SD for n = 2. Total area is sum of area under indicated protein band curves in the elution lane.

Figure S7. Microscale thermophoresis (MST) using fluorescent label (FL) on different binding partners can be used to analyze binding interactions between DnaK and DnaJ2. (a) Initial fluorescence measurements of MST samples containing DnaJ2-FL (21 nM) with varying concentration of wt or mutant DnaK (defective in hydrolyzing ATP) in the

presence of 2 mM ATP/$MgCl_2$. In order to perform MST analysis, the initial fluorescence must be +/-10% of the average for all samples, as shown by the dotted lines for DnaK (T175S). Wild-type DnaK samples do not fall within the +/-10% cutoff, perhaps because of conformational changes in DnaJ2-FL as it binds/releases DnaK during ATP hydrolysis. (b) MST analysis of wild-type DnaK-FL (30 nM) with a range of wild-type DnaJ2 in the absence of nucleotide. The initial fluorescence of each sample was within the +/-10% range. (c) ATPase activity analysis of indicated concentrations of DnaK with and without FL in the presence of cofactors shows that labeling does not affect the activity of DnaK. (d) ATPase activity of DnaK stimulated by indicated concentration of DnaJ2 with and without FL shows that labeling does slightly affect the amount of activation, but DnaJ2-FL is still active. For a-b, error bars indicate SD for n = 2; for c-d, error bars indicate SEM for n = 2.

Figure S8. Recombinant Mtb ClpB forms oligomers and exhibits ATPase activity *in vitro*. (a) Gel filtration UV trace of Mtb ClpB in the presence and absence of ATP using a published protocol to evaluate its oligomeric state. ClpB (4 mg) was injected on a superdex 200 10/300 GL column in 50 mM Tris (pH 7.5), 0.2 M KCl, 20 mM $MgCl_2$, 1 mM EDTA, 1 mM DTT, 10% (vol/vol) glycerol +/- 2 mM ATP.(1) HMW protein standards (GE Healthcare) were injected on the same column using the same buffers. The elution volume of the standards was not affected by the addition of ATP; however, ClpB eluted at a lower volume in ATP signifying a shift to a higher oligomeric state as indicated in the table (right). (b) Gel filtration UV trace of a higher concentration of Mtb ClpB (2x of that shown in part a) in 20 mM tris (pH 8.0), 150 mM NaCl, 10% (vol/vol) glycerol for use in enzymatic assays. Fractions corresponding to the major peak between 10-12 mL elution volume were collected. For parts a and b, the oligomeric state of ClpB was estimated based on the elution volume of the standards in the appropriate buffer using the manufacturer's instructions, see *Methods* section (GE Healthcare). (c) ATPase activity of ClpB purified from part b at indicated concentrations at t = 20 min (error bars indicate SD for n =2).

Figure S9. Mtb Hsp20 (Rv0251c) helps re-solubilize heat-aggregated luciferase *in vitro*. (a) Representative western blot (anti-luciferase) of 25 nM luciferase +/- Hsp20 (100 nM) that is untreated (native) or heat-treated at 42°C for 10 min (denatured) prior to ultracentrifugation to separate soluble (S/N) and pellet (P) fractions. (b) Analysis of

samples from part a. Luciferase activity of samples measured before ultracentrifugation, which illustrates that denatured luciferase is heat killed with or without Hsp20 (left). Quantification of western blots shows the percent of luciferase in each fraction for the indicated samples, showing that there is slightly more soluble heat-killed luciferase in samples containing Hsp20 (compare denatured sample +/- Hsp20) (right). (c) Titration of Hsp20 to luciferase (25 nM) prior to heat-treatment shows that the efficiency of the refolding reaction by DnaK + ClpB and cofactors improves with increasing [Hsp20] (reaction performed as described for Figure 4, read at t = 60 min). Four-fold Hsp20 was chosen for experiments because it allows us to distinguish between chaperone reactions +/- ClpB. For part b, error bars indicate SD for n = 2. For part c, error bars indicate SEM for n = 2. Western blots were quantified using Image J. Note that the gel shift in the aggregated luciferase versus native fractions is likely due to the tendency of protein aggregates or unfolded structures to migrate less efficiently by gel electrophoresis (see ref (2, 3)) and the presence of another detergent in the aggregate re-solubilization buffer.

Figure S10. Normalization of heat-treated luciferase refolding data demonstrates consistent results when different stocks of luciferase are used. Over the course of performing luciferase refolding experiments, there were differences in the native luciferase activity depending on the stock of enzyme used, which resulted in different "percent luciferase activity" values for similar reaction mixtures. This graph shows that when the data of independent luciferase refolding experiments is first normalized and then combined, there is low error. We present the data in the remainder of the figures as "percent native luciferase" because these experiments were done using native luciferase with similar activities. Shown here, after heat-treatment of 25 nM luciferase with 100 nM Hsp20, reactions were conducted at 25 °C containing 4 μM DnaK, 2 μM ClpB, 2 μM GrpE and 2 μM each J-protein, and were read at t = 30 min. Error bars indicate SEM for n = 4.

Figure S11. Refolding of heat-treated luciferase by DnaK, ClpB and GrpE with varying [J-protein] using wild-type and HPD motif mutants demonstrates inhibition of the reaction with J-protein mutants. (a) Percent of active luciferase resulting from reactions containing increasing amounts of one J-protein shows that increased concentration of either J1 or J2 does not refold as efficiently as both J1 and J2. (b) Addition of DnaJ2(H32Q) to refolding reactions containing only one J-protein (DnaJ2) shows that

the point mutant inhibits the reaction in a concentration dependent manner. The point mutant alone demonstrates no cofactor activity, even at high concentration (light blue bar). (c) Addition of increasing wild-type DnaJ1 to refolding reactions containing both DnaJ1 and J2 does not affect refolding, while increasing [DnaJ1(H38Q)] inhibits the reaction in a concentration-dependent manner. After heat-treatment of 25 nM luciferase with 100 nM Hsp20, all reactions were conducted at 25 °C containing 4 μM DnaK, 2 μM ClpB, 2 μM GrpE and the indicated amount of J-protein, and were read at t = 30 min. Error bars indicate SEM for n = 2. D.L. is denatured luciferase starting material.

Figure S12. DnaJ2-mediated stimulation of DnaK's ATPase activity is stronger than DnaJ1-mediated stimulation in the presence and absence of aggregated substrate. ATPase activity was measured as described in the Methods section, except indicated proteins (4 μM DnaK and 400 nM each cofactor) were incubated with denatured luciferase plus Hsp20 (25 and 100 nM, respectively) in Buffer H (D.L.) or just Buffer H alone, for 10 min at 37 °C prior to initiation with 100 μM ATP. Note that the baseline activity of DnaK is slightly higher than that seen in Figure 2a, likely due to the presence of Buffer H.

Figure S13. DnaJ2(H32Q) partially inhibits activation of DnaK's ATPase activity by sub-stoichiometric DnaJ2 and GrpE at concentrations similar to those used in Figure 4e. DnaK (4 μM) was incubated with DnaJ2 (1 μM) and GrpE (400 nM) with indicated concentrations of additional wild-type or mutant DnaJ2 prior to addition of 100 μM ATP at 37 °C. The red dashed line indicates the initial rate with only DnaK and GrpE, representing full inhibition of the DnaJ2-induced activation. The black dashed line indicates the initial rate with 1 μM DnaJ2 added. Error bars indicate SEM for n=2.

Figure S14. Southern blot confirmation of *M. smegmatis* (Msm) *dnaJ1* and *dnaJ2* allelic replacements. Expected band sizes indicated at left of blot. (a) Confirmation of *dnaJ1* deletion using AhdI/ClaI double digest of genomic DNA and *dnaJ1* 5′ flank as probe. Ladder (1500bp), wildtype (3436bp), MGM6272 (*ΔdnaJ1 attB:Pmop-dnaJ1 kan*) and MGM6239 (*ΔdnaJ1 ΔdnaJ2:hyg* attB:Pmop-dnaJ1 strep) (2263bp). (b) Confirmation of *dnaJ2* deletion using MluI/MscI double digest of genomic DNA and *dnaJ2* 5′ flank as

probe. Ladder (1500bp), wildtype (2198bp), MGM6070 (Δ*dnaJ2*::*hyg*)and MGM6239 (*ΔdnaJ1 ΔdnaJ2:hyg attB:Pmop-dnaJ1 strep*), (2726bp).

Figure S15. Msm single *dnaJ* deletion mutants are *not* more sensitive to heat or aggregate-forming antibiotics than wild-type. (a) Heat sensitivity of *mc²155* (wild-type), MGM6069 (*ΔdnaJ1 attB::strep*), and MGM6070 (*ΔdnaJ2::loxP-hyg*). Cultures at OD_{600} 0.4 were incubated at 53°C. Aliquots were taken at indicated time points and serial dilutions were plated on LBsmeg. (b) MIC determination by pellicle formation in the presence of isoniazid (INH) and kanamycin of *mc²155* (wild-type), MGM6069 (*ΔdnaJ1 attB::strep*), and MGM6160 (*ΔdnaJ2::loxP-hyg attB::strep*), and complemented strains MGM6272 (*ΔdnaJ1 attB::Pmop-dnaJ1 strep*) and MGM6161 (*ΔdnaJ2::loxP-hyg attB::Pmop-dnaJ2 strep*). See description of MIC method above.

Figure S16. Msm (Ms) *dnaJ* is essential for growth. Strains carrying deletions in chromosomal *dnaJ1 and dnaJ2* and a copy of *dnaJ1* at the *attB* phage integration site were subjected to marker exchange with *attB* integrating vectors. (A) Δ*dnaJ1* Δ*dnaJ2::hyg attB::Pmop-dnaJ1 kan* (MGM6240) transformed with pDB60 ($strep^R$, empty vector) or pAJF295 (Ms *dnaJ1*), pAJF296 (Ms *dnaJ2*), pAJF710 (Mtb *dnaJ2*), pAJF700 (Ms *dnaJ2 H32Q*), pAJF705 (Mtb *dnaJ1 H38Q*), or pAJF707 (Mtb *dnaJ2 H32Q*). Transformations were plated on streptomycin selective media incubated at 37°C . (B) *ΔdnaJ1 ΔdnaJ2::hyg attB::Pmop-dnaJ1 kan* (MGM6240) transformed with pDB60 (empty vector), pAJF710 (Mtb *dnaJ2*), or pAJF707 (Mtb *dnaJ2 H32Q*). Transformations were plated on streptomycin selective media incubated at 30°C

Figure S17. Western blot of DnaJ proteins in Msm. (a) Lysates from DnaJ1 mutants in Msm, MGM6272 *(*Δ*dnaJ1* attB::Pmop-*dnaJ1* strep), MGM6069 (Δ*dnaJ1 attB*::strep), MGM6284, (Δ*dnaJ1 attB*::Pmop-Ms*dnaJ1*(H38Q) strep), and MGM6283 (Δ*dnaJ1* attB::Pmop-Mtb *dnaJ1*(H38Q) strep) probed for DnaJ1 (top) and RNAP Beta (bottom). (b) Lysates from DnaJ2 mutants in Msm*,* MGM6161 *(*Δ*dnaJ2*::*hyg attB::Pmop-MsdnaJ2 strep),* MGM6160 *(*Δ*dnaJ2*::*hyg attB:strep),* MGM6285 *(ΔdnaJ2*::*hyg attB*::*Pmop-Ms dnaJ2(H32Q) strep), and* MGM6286 *(*Δ*dnaJ2*::*hyg attB*::*Pmop-MtbdnaJ2(H32Q) strep)* probed for DnaJ2 (top) and RNAP Beta (bottom)

Figure S1.

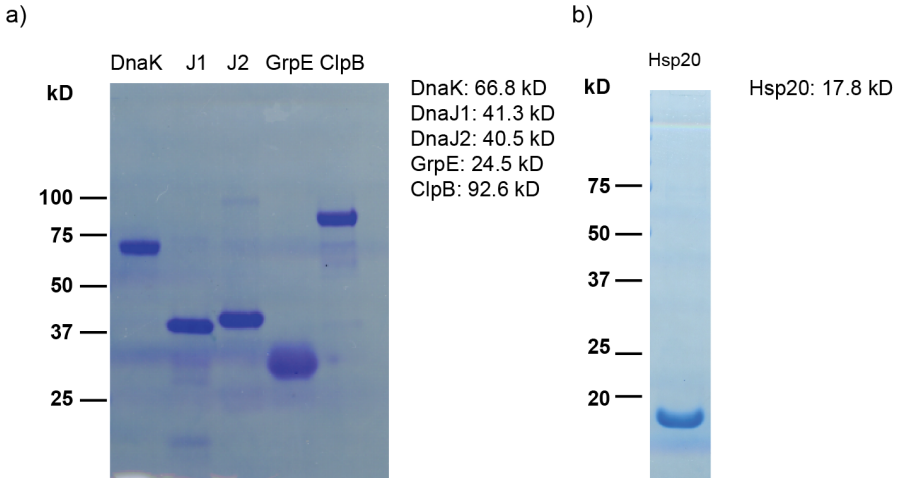

Figure S2.

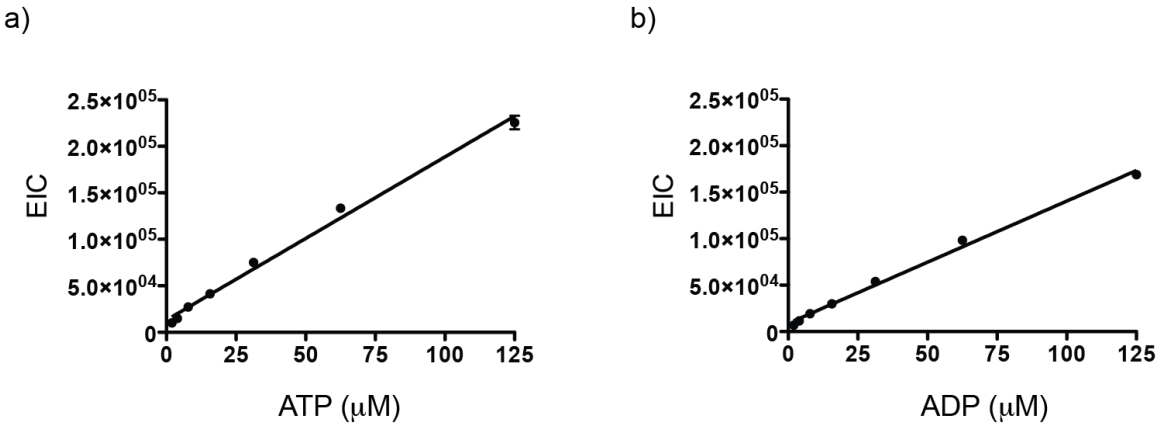

Figure S3.

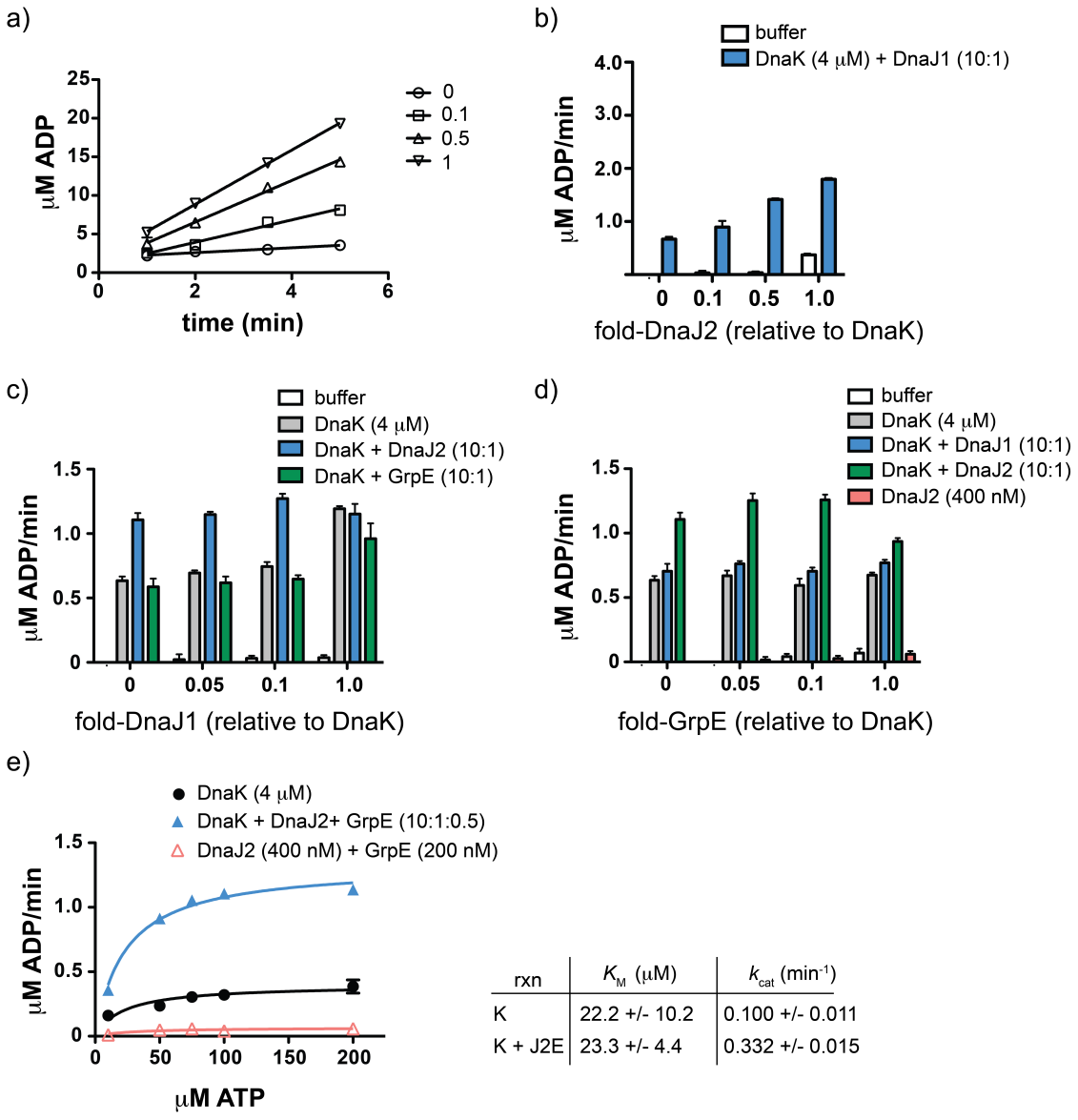

rxn	K_M (μM)	k_{cat} (min^{-1})
K	22.2 +/- 10.2	0.100 +/- 0.011
K + J2E	23.3 +/- 4.4	0.332 +/- 0.015

Figure S4.

```
sp|P9WNV7|DNAJ2_MYCTU ------MARDYYGLLGVSKNASDADIKRAYRKLARELHPDVNP-DEAAQAKFKEISVAYE
tr|A0R0T8|DNAJ2_MYCS2 ------MARDYYGLLGVSKGASDSEIKRAYRRLARELHPDVNP-DEEAQHRFTEIQQAYE
sp|P08622|DNAJ_ECOLI  -----MAKQDYYEILGVSKTAEEREIRKAYKRLAMKYHPDRNQGDKEAEAKFKEIKEAYE
sp|P9WNV9|DNAJ1_MYCTU MAQREWVEKDFYQELGVSSDASPEEIKRAYRKLARDLHPDANPGNPAAGERFKAVSEAHN
tr|A0QQD0|DNAJ1_MYCS2 MAQREWVEKDFYKELGVSSDASADEIKKAYRKLAAELHPDRNS-DPGAAERFKAVSEANS
sp|P25685|DNJB1_HUMAN ------MGKDYYQTLGLARGASDEEIKRAYRRQALRYHPDKNK-EPGAEEKFKEIAEAYD
sp|P25491|YDJ1_YEAST  ----MVKETKFYDILGVPVTATDVEIKKAYRKCALKYHPDKNP-SEEAAEKFKEASAAYE
sp|O60884|DNJA2_HUMAN --MANVADTKLYDILGVPPGASENELKKAYRKLAKEYHPDKNP-N--AGDKFKEISFAYE
                              . *  **:   *   ::::**:: *   *** *  .  *  :*.    * .
```

Figure S5.

a)

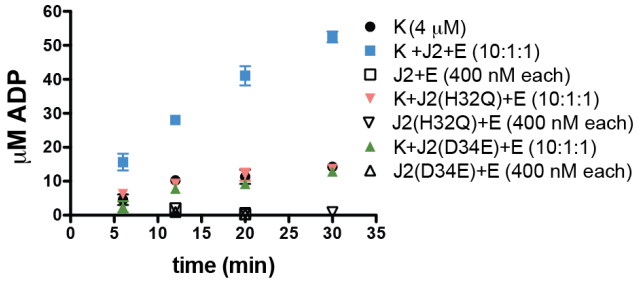

b)

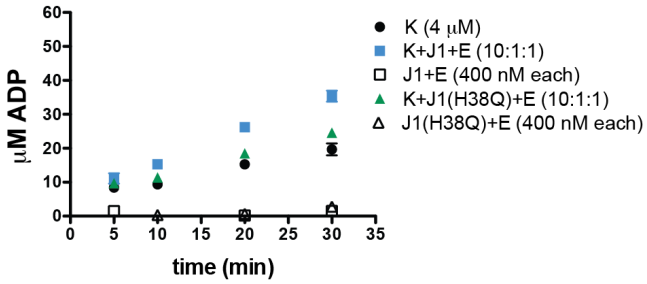

Figure S6:

a)

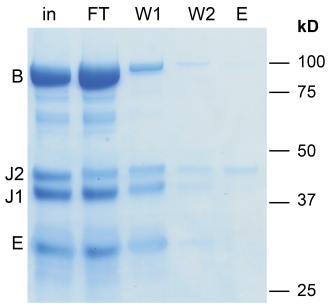

b)

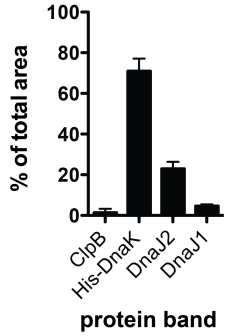

c)

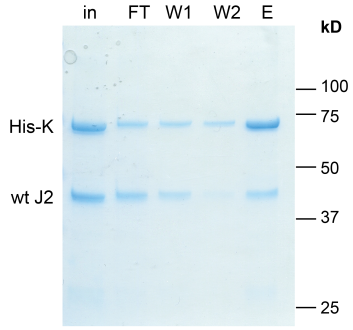

d)

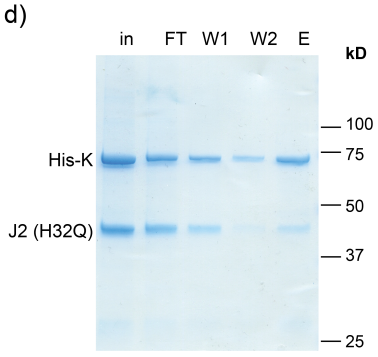

e)

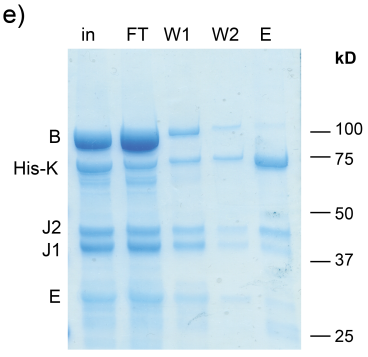

f)

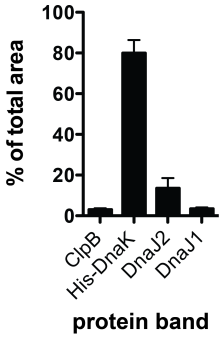

Figure S7.

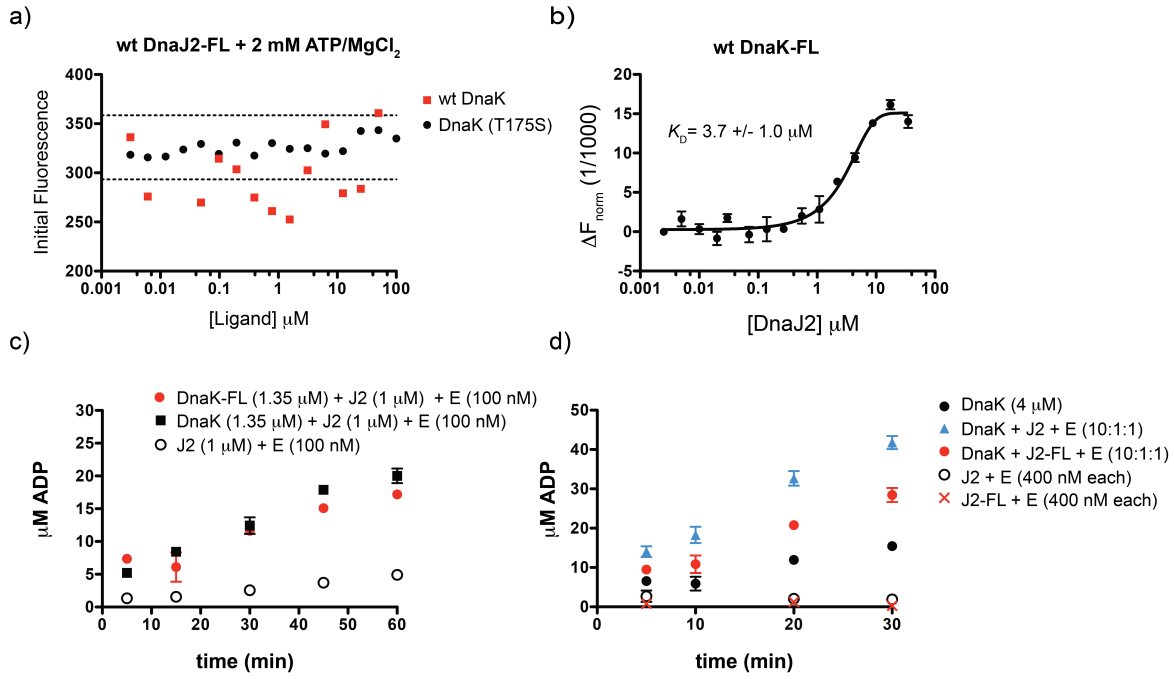
a)
wt DnaJ2-FL + 2 mM ATP/MgCl2
Initial Fluorescence
[Ligand] μM
wt DnaK
DnaK (T175S)
b)
wt DnaK-FL
KD= 3.7 +/- 1.0 μM
ΔFnorm (1/1000)
[DnaJ2] μM
c)
DnaK-FL (1.35 μM) + J2 (1 μM) + E (100 nM)
DnaK (1.35 μM) + J2 (1 μM) + E (100 nM)
J2 (1 μM) + E (100 nM)
μM ADP
time (min)
d)
DnaK (4 μM)
DnaK + J2 + E (10:1:1)
DnaK + J2-FL + E (10:1:1)
J2 + E (400 nM each)
J2-FL + E (400 nM each)
μM ADP
time (min)

Figure S8.

a)

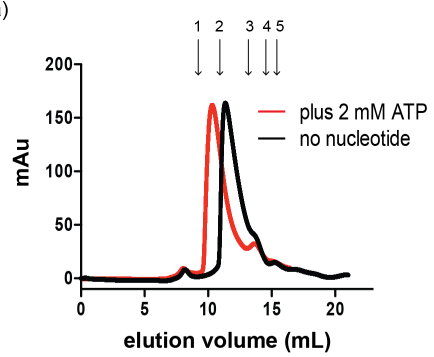

stand.	MW (kD)	elution vol (mL) +ATP	-ATP
1	669	9.4	9.4
2	440	11.0	11.1
3	158	13.2	13.2
4	75	14.5	14.5
5	44	15.4	15.5

sample	vol (mL)	pred. MW (kD)	pred. ClpB units
ClpB + ATP	10.3	521.1	5.6
ClpB - ATP	11.3	332.4	3.6

b)

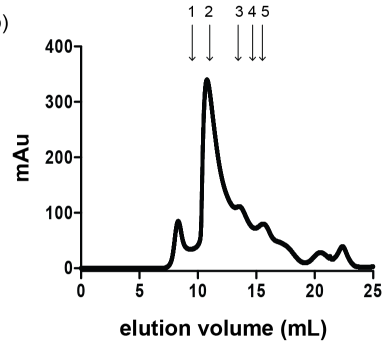

stand.	MW (kD)	elution vol (mL)
1	669	9.7
2	440	11.0
3	158	13.5
4	75	14.7
5	44	15.5

sample	vol (mL)	pred. MW (kD)	pred. ClpB units
ClpB (8 mg)	10.8	466.7	5.0

c)

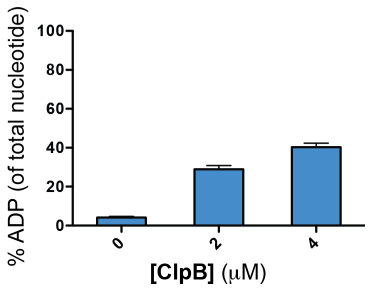

Figure S9.

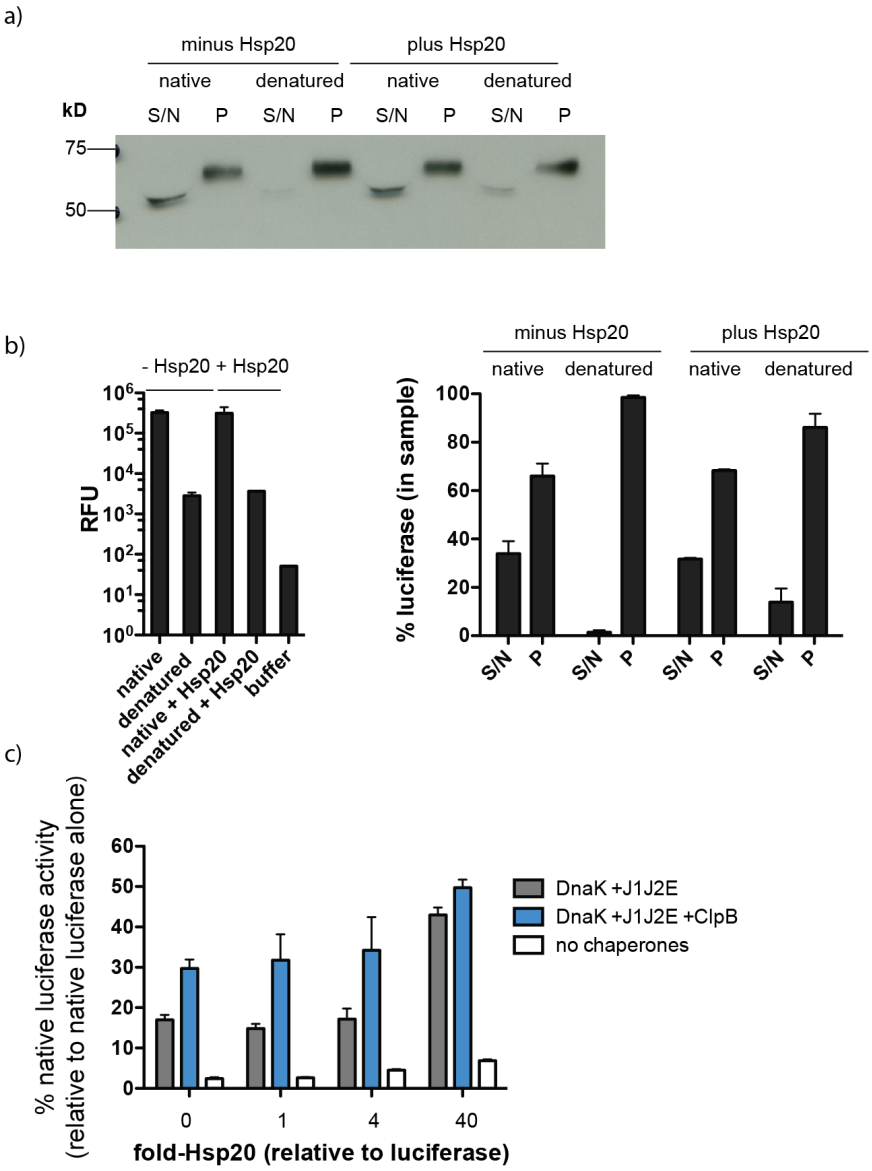
a)
minus Hsp20
plus Hsp20
native
denatured
native
denatured
kD
S/N
P
S/N
P
S/N
P
S/N
P
75
50
b)
- Hsp20 + Hsp20
RFU
native
denatured
native + Hsp20
denatured + Hsp20
buffer
minus Hsp20
plus Hsp20
native
denatured
native
denatured
% luciferase (in sample)
S/N
P
S/N
P
S/N
P
S/N
P
c)
% native luciferase activity
(relative to native luciferase alone)
DnaK +J1J2E
DnaK +J1J2E +ClpB
no chaperones
fold-Hsp20 (relative to luciferase)

Figure S10.

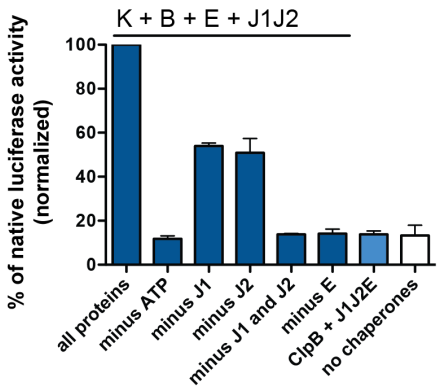

Figure S11.

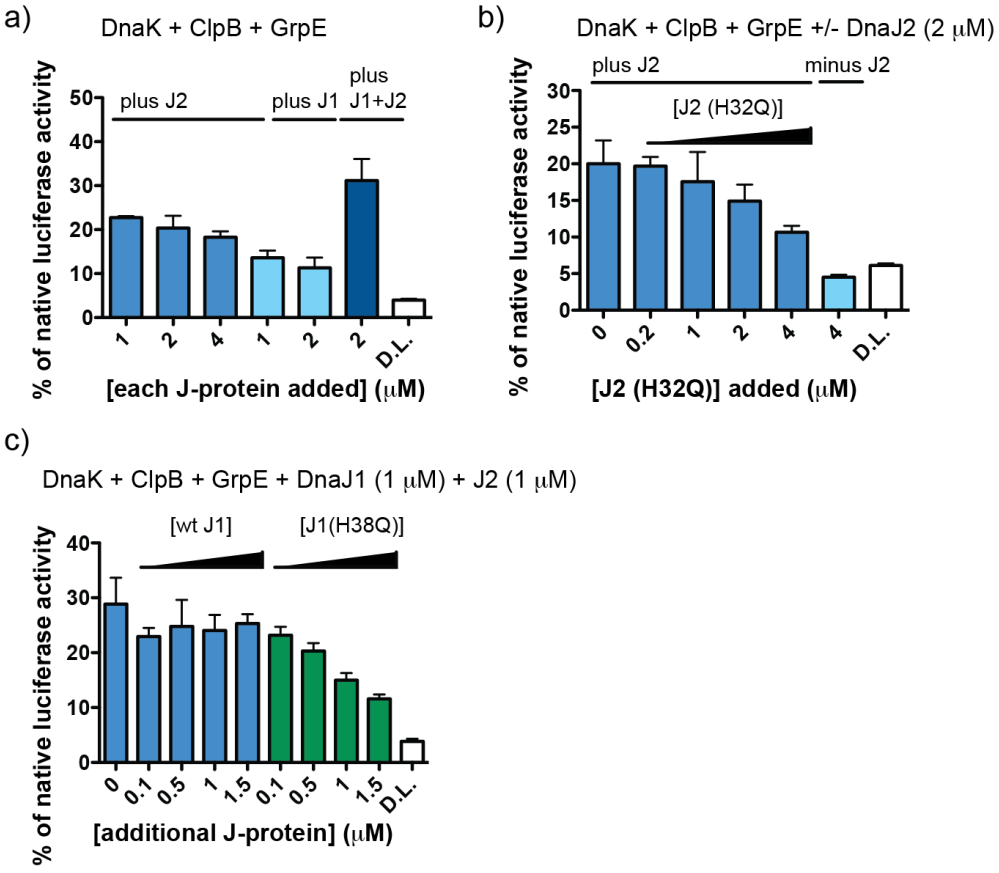

Figure S12.

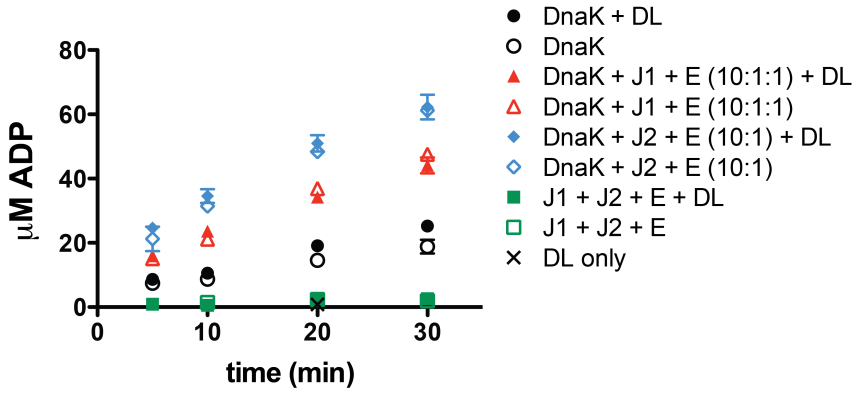

Figure S13.

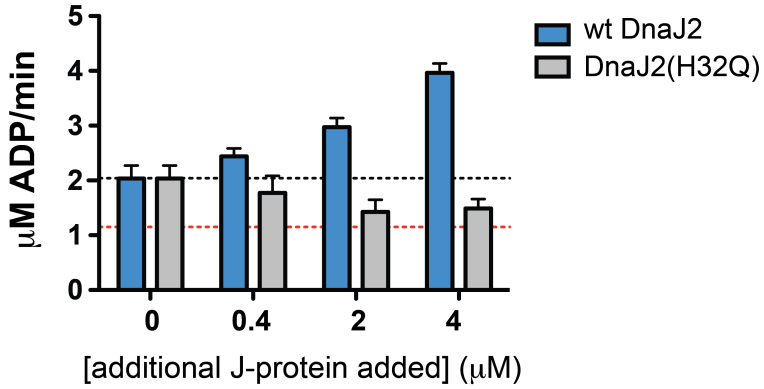

Figure S14.

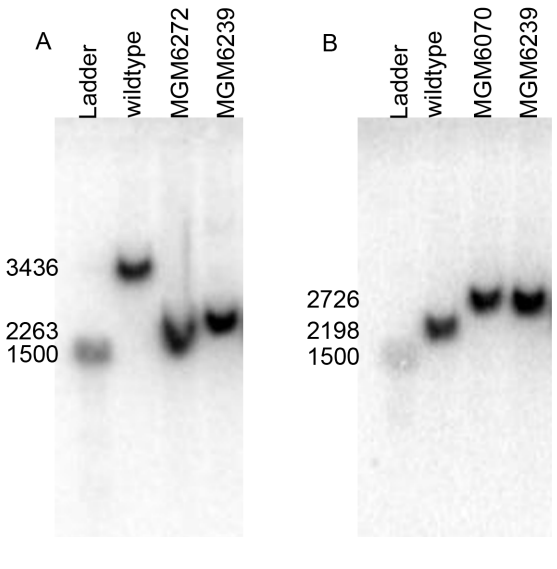

Figure S15.

a)

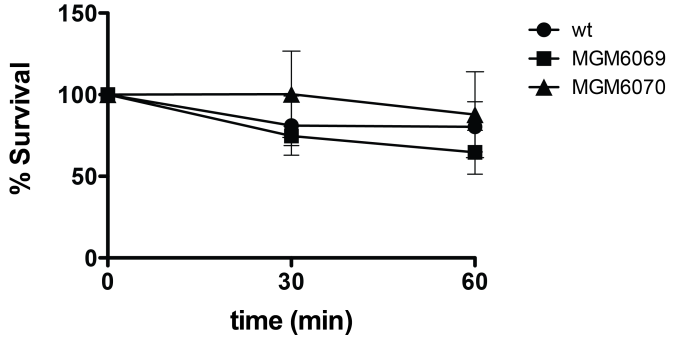

b)

	MIC (μg/mL)	
strain	INH	kanamycin
mc2155	5-10	0.625-1.25
MGM6069	5-10	0.625-1.25
MGM6160	5-10	0.625-1.25
MGM6272	5-10	0.625-1.25
MGM6161	5-10	0.625-1.25

Figure S16.

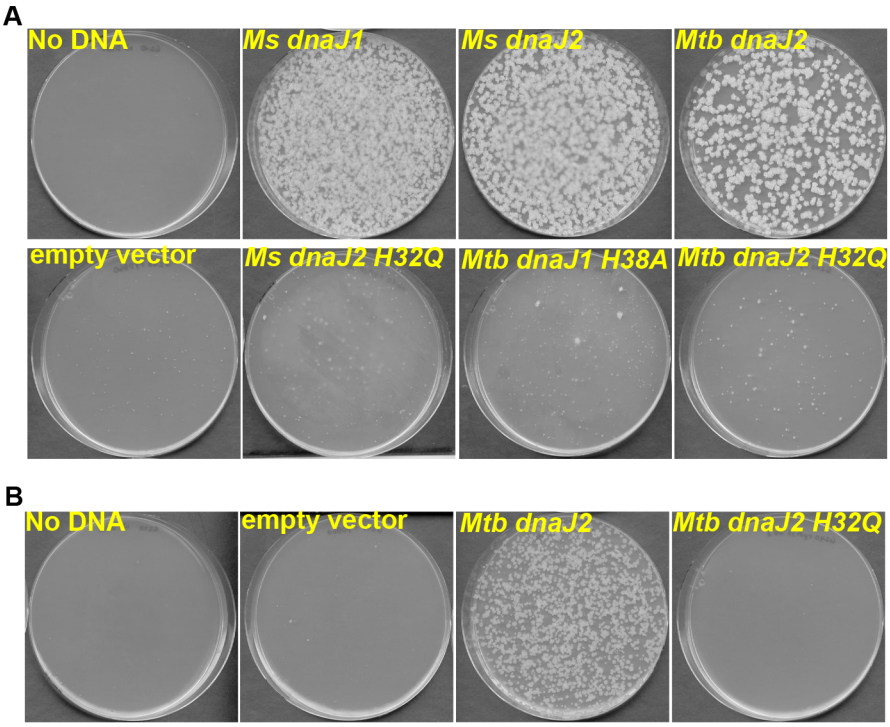

Figure S17.

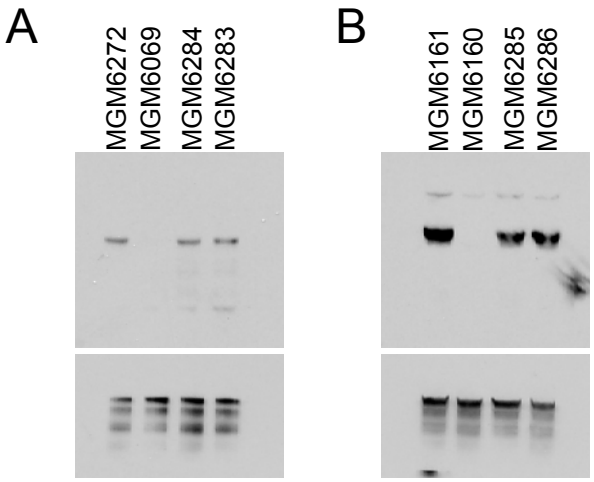
A
MGM6272
MGM6069
MGM6284
MGM6283
B
MGM6161
MGM6160
MGM6285
MGM6286

Table S1. Strains used in this study.

Strain Name	***Genotype***	**Details of Construction**
Rosetta2	*E. coli* BL21 derivative for rare codon usage	Novagen
Rosetta2(DE3) pLysS	Rosetta2 expressing T7 lysozyme	Novagen
EcTL02	His6-SUMO-Mtb clpB	Rosetta2 transformed with pEcTL02
EcTL03	His6-SUMO-Mtb dnaJ1	Rosetta2 transformed with pEcTL03
EcTL04	His6-SUMO-Mtb dnaJ2	Rosetta2 transformed with pEcTL04
EcTL05	His6-SUMO-Mtb grpE	Rosetta2 transformed with pEcTL05
EcTL06	His6-SUMO-Mtb dnaK	Rosetta2 transformed with pEcTL06
EcTL07	His6-Mtb dnaK	Rosetta2 transformed with pEcTL07
EcTL08	His6-Mtb-Hsp20	Rosetta2 transformed with pEcTL08
EcTL09	His6-SUMO-Mtb dnaK(T175S)	Rosetta2 transformed with pEcTL09
EcTL10	His6-SUMO-Mtb dnaJ1(H38Q)	Rosetta2 transformed with pEcTL10
EcTL11	His6-SUMO-Mtb dnaJ1(D40E)	Rosetta2 transformed with pEcTL11
EcTL12	His6-SUMO-Mtb dnaJ2(H32Q)	Rosetta2 transformed with pEcTL12
EcTL13	His6-SUMO-Mtb dnaJ2(D34E)	Rosetta2 transformed with pEcTL13
EcTL14	His6-Ulp1 (residues 403-621)	Rosetta2(DE3)pLysS transformed with pHYRS52
mc2155	wildtype *M. smegmatis*	**ref. (4)**
MGM6069	*ΔdnaJ1 attB::strep*	*dnaJ1* knockout made with pAJF258 containing pDB60 in mc2155
MGM6070	*ΔdnaJ2::loxP-hyg*	*dnaJ2* knockout made with temperature sensitive phage using pAJF306 in mc2155
MGM6160	*ΔdnaJ2::loxP-hyg attB::strep*	MGM6070 transformed with pDB60
MGM6161	*ΔdnaJ2::loxP-hyg attB::Pmop-dnaJ2 strep*	MGM6070 transformed with pAJF296
MGM6239	*ΔdnaJ1 ΔdnaJ2::loxP-hyg attB::Pmop-dnaJ1 strep*	MGM6240 transformed with pAJF295
MGM6240	*ΔdnaJ1 ΔdnaJ2::loxP-hyg attB::Pmop-dnaJ1 kan*	MGM6241 with dnaJ2 knockout made with temperature sensitive phage using pAJF306
MGM6241	*ΔdnaJ1 attB::Pmop-dnaJ1 kan*	MGM6069 transformed with pAJF260
MGM6272	*ΔdnaJ1 attB::Pmop-dnaJ1 strep*	MGM6241 transformed with pAJF295
MGM6282	*ΔdnaJ1 ΔdnaJ2::loxP-hyg attB::zeo pAJF329*	MGM6239 transformed with pDB19 and pAJF329
MGM6283	*ΔdnaJ1 attB::Pmop-Mtb dnaJ1(H38Q) strep*	MGM6241 transformed with pAJF705
MGM6284	*ΔdnaJ1 attB::Pmop-Ms dnaJ1(H38Q) strep*	MGM6241 transformed with pAJF738
MGM6285	*ΔdnaJ2::loxP-hyg attB::Pmop-Ms dnaJ2(H32Q) strep*	MGM6070 transformed with pAJF700
MGM6286	*ΔdnaJ2::loxP-hyg attB::Pmop-Mtb dnaJ2(H32Q) strep*	MGM6070 transformed with pAJF707

Table S2. Plasmids used in this study

Plasmid name	Relevant features	Construction
pETHisSUMO	pET His6 Sumo TEV LIC cloning vector carb	Addgene #29711
pHYRS52	His6-*S. cerevisiae* ulp1 (res. 403-621) carb	Addgene #31122 **(ref (5))**
pET-47b(+)	N-terminal His6 kan	Novagen
pEcTL02	His6-SUMO-Mtb clpB	overlap extension PCR with pETHisSUMO and megaprimer made using oClpBf and oClpBr
pEcTL03	His6-SUMO-Mtb dnaJ1	overlap extension PCR with pETHisSUMO and megaprimer made using oDnaJ1f and oDnaJ1r
pEcTL04	His6-SUMO-Mtb dnaJ2	overlap extension PCR with pETHisSUMO and megaprimer made using oDnaJ2f and oDnaJ2r
pEcTL05	His6-SUMO-Mtb grpE	overlap extension PCR with pETHisSUMO and megaprimer made using oGrpEf and oGrpEr
pEcTL06	His6-SUMO-Mtb dnaK	overlap extension PCR with pETHisSUMO and megaprimer made using oDnaKf and oDnaKr
pEcTL07	His6-Mtb dnaK	mutagenesis of pEcTL06 using oMutDnaKf and oMutDnaKr
pEcTL08	His6-Mtb-Hsp20	overlap extension PCR with pET47b and megaprimer made using oHspf and oHspr
pEcTL09	His6-SUMO-Mtb dnaK(T175S)	mutagenesis of pEcTL06 using oMutT175Sf and oMutT175Sr
pEcTL10	His6-SUMO-Mtb dnaJ1(H38Q)	mutagenesis of pEcTL03 using oMutH38Qf and oMuttH38Qr
pEcTL11	His6-SUMO-Mtb dnaJ1(D40E)	mutagenesis of pEcTL03 using oMutD40Ef and oMuttD40Er
pEcTL12	His6-SUMO-Mtb dnaJ2(H32Q)	mutagenesis of pEcTL04 using oMutH32Qf and oMuttH32Qr
pEcTL13	His6-SUMO-Mtb dnaJ2(D34E)	mutagenesis of pEcTL03 using oMutD34Ef and oMuttD34Er
pDB19	attP(L5)::zeo	Lab Stock
pDB60	attP(L5)::strep	Lab Stock
pmsg419	P_{Tb21}-tetR(sB) $P_{myc1\text{-}tetO}$-HA hyg oriM	Lab Stock
pMV306kn	attP(L5)::kan	Lab Stock
pAJF067	hyg, galK, sacB	**ref (2)**
pAJF256	Ms dnaJ1 knockout front flank, sacB, galK, hyg	cut Msmeg_0711 front flank (oAF318/oAF319, MC2155 gDNA) with SpeI/NdeI and ligated to pAJF067 cut with same
pAJF258	Ms dnaJ1 knockout front flank and back flank, sacB, galK, hyg	cut Msmeg_0711 back flank (oAF320/oAF321, MC2155 gDNA) with AvrII/NdeI and ligated to pAJF256 cut with same
pAJF260	attB:Pmop-Ms dnaJ1 kan	cut Msmeg_0711 (oAF328/oAF329, MC2155 gDNA) with NdeI/ClaI and ligating to pAJF070
pAJF261	attB:Pmop-Ms dnaJ2 kan	cut Msmeg_4504 (oAF326/oAF327, MC2155 gDNA) with NdeI/ClaI and ligating to pAJF070
pAJF295	attB:Pmop-Ms dnaJ1 strep	cut Pmop-dnaJ1 from pAJF260 with XbaI/ClaI and ligated to pDB60 cut with same
pAJF296	attB:Pmop-Ms dnaJ2 strep	cut Pmop-dnaJ2 from pAJF261 with XbaI/ClaI and ligated to pDB60 cut with same
pAJF304	pmsg360hyg plus Ms dnaJ2 front flank	cut dnaJ2 front flank (oAF389/oAF390, MC2155 gDNA) with BglII/HindIII and ligated to pmsg360hyg cut with same

pAJF306	Ms dnaJ2 phage KO vector	cut dnaJ2 back flank (oAF391/oAF392, MC2155 gDNA) with XbaI/BamHI and ligating to pAJF304 cut with same
pAJF329	PTb21-tetR(sB), Pmyc1tetO-HA-dnaJ2, kan, oriM	cut dnaJ2 (oAF418/oAF419, MC2155 gDNA) with ClaI/AclI and ligated to pAJF326 cut with same
pAJF700	attB:Pmop-Ms dnaJ2(H32Q) strep	in-fusion reaction of pDB60 linearized with XbaI/ClaI and 5'dnaJ2H32Q (306knfwd/oAF1262, pAJF296) and 3'dnaJ2H32Q (oAF765/oAF1263, pAJF296)
pAJF705	attB:Pmop-Mtb dnaJ1(H38Q) strep	in-fusion reaction of 5'dnaJ1 (oAF1250/1254, Mtb gDNA), 3'dnaJ1 (oAF1255/1251, Mtb gDNA) and pAJF296 linearized with NdeI/ClaI
pAJF706	attB:Pmop-Mtb dnaJ1(D40E) strep	in-fusion reaction of 5'dnaJ1 (oAF1250/1256, Mtb gDNA), 3'dnaJ1 (oAF1257/1251, Mtb gDNA) and pAJF296 linearized with NdeI/ClaI
pAJF707	attB:Pmop-Mtb dnaJ2(H32Q) strep	in-fusion reaction of 5'dnaJ2 (oAF1252/1258, Mtb gDNA), 3'dnaJ2 (oAF1259/1253, Mtb gDNA) and pAJF296 linearized with NdeI/ClaI
pAJF708	attB:Pmop-Mtb dnaJ2(D34E) strep	in-fusion reaction of 5'dnaJ2 (oAF1252/1260, Mtb gDNA), 3'dnaJ2 (oAF1261/1253, Mtb gDNA) and pAJF296 linearized with NdeI/ClaI
pAJF710	attB(L5):Pmop-Mtb dnaJ2 strep	in-fusion reaction of Mtb dnaJ2 (oAF1252/1253, Mtb gDNA) and pAJF296 linearized with NdeI/ClaI
pAJF738	attB:Pmop-Ms dnaJ1(H38Q) strep	in-fusion reaction of 5'dnaJ1 (306knfwd/oAF1301, pAJF260), 3'dnaJ1 (oAF1302/765, pAJF685) and pDB60 linearized with XbaI/ClaI

Table S3. Oligonucleotides used for this study

Oligo name	5'-3' sequence
oClpBf	GAGGCTCACAGAGAACAGATTGGTGGGGTGGACTCGTTTAACCCGAC
oClpBr	CTTTCGGGCTTTGTTAGCAGCCGGATCAGTCAGCCCAGGATCAGCGAGTC
oDnaJ1f	GAGGCTCACAGAGAACAGATTGGTGGGATGGCCCAAAGGGAATGGGTC
oDnaJ1r	CTTTCGGGCTTTGTTAGCAGCCGGATCAGTCAGCGATTACCTGCCCATCCG
oDnaJ2f	GAGGCTCACAGAGAACAGATTGGTGGGGTGGCACGCGATTATTACGG
oDnaJ2r	CTTTCGGGCTTTGTTAGCAGCCGGATCAGTTAGCGCCCGGTGAAGGTCT
oGrpEf	GAGGCTCACAGAGAACAGATTGGTGGGGTGACGGACGGAAATCAAAAGC
oGrpEr	CTTTCGGGCTTTGTTAGCAGCCGGATCAGTTAACTGCCCGACGGTTCTG
oDnaKf	GAGGCTCACAGAGAACAGATTGGTGGGATGGCTCGTGCGGTCGGGATCGACCTC
oDnaKr	CTTTCGGGCTTTGTTAGCAGCCGGATCAGTCACTTGGCCTCCCG
oMutDnaKf	ATGGTTCTTCTATGGCTAGCATGGCTCGTGCGGTCGGGAT
oMutDnaKr	ATCCCGACCGCACGAGCCATGCTAGCCATAGAAGAACCAT
oHspf	CGGCTCTTGAAGTCCTCTTTCAGGGACCCATGAACAATCTCGCATTGTGGTCGCGTC
oHspr	TTCTTTACTACCGCGTGGCACCAGAGCGAGCTACTTCGTGATGGCGATGCGCTGC
oMutT175Sf	CGACTTGGGTGGTGGCAGTTTCGACGTTTCCCTG
oMutT175Sr	CAGGGAAACGTCGAAACTGCCACCACCCAAGTCG
oMutH38Qf	CGCGCGACCTGCAACCGGACGCGAACCCGGGCAAC
oMutH38Qr	GTTGCCCGGGTTCGCGTCCGGTTGCAGGTCGCGCG
oMutD40Ef	CGCGCGACCTGCATCCGGAAGCGAACCCGGGCAAC
oMutD40Er	GTTGCCCGGGTTCGCTTCCGGATGCAGGTCGCGCG
oMutH32Qf	CTGGCGCGCGAGCTGCAACCCGACGTCAACCCGGACGAG
oMutH32Qr	CTCGTCCGGGTTGACGTCGGGTTGCAGCTCGCGCGCCAG
oMutD34Ef	CTGGCGCGCGAGCTGCATCCCGAAGTCAACCCGGACGAG
oMutD34Er	CTCGTCCGGGTTGACTTCGGGATGCAGCTCGCGCGCCAG
oAF318	GTTACTAGTCCCGCAAGGGTCGGCG21
oAF319	GCACATATGGCTGCGCCACCTCCTTAC
oAF320	GTACATATGTGAGCGGCAAACGCAAC21
oAF321	GTTCCTAGGAGCGGCGTGACCGCGTC
oAF326	GTTCATATGACCCGGCACAGAAAGG
oAF327	GACATCGATTCAGCGACCGGTGAAC
oAF328	GTCCATATGTAGAAAGAAGAGGTAAG
oAF329	GACATCGATTCATACATTCCCCGCCCATC
oAF389	GTTAGATCTTCGGCGACGCGATCGACG
oAF389	GTTAGATCTTCGGCGACGCGATCGACG
oAF390	GTTAAGCTTGCTGTCTTGCCTGACC
oAF390	GTTAAGCTTGCTGTCTTGCCTGACC
oAF391	GAATCTAGATGACGGACGTGGGCG
oAF392	GAAGGATCCGACAGGTATTTCGGCG
oAF418	GTTATCGATTCGGCACGTGATTACTAC

oAF419	GTTAACGTTCAGCGACCGGTGAACG
oAF1254	GTCCGGTTGCAGGTCGCGCGCCAAC
oAF1255	GACCTGCAACCGGACGCGAACCCGG
oAF1256	GGTTCGCTTCCGGATGCAGGTCGCG
oAF1257	CATCCGGAAGCGAACCCGGGCAACC
oAF1258	CGTCGGGTTGCAGCTCGCGCGCCAG
oAF1259	GAGCTGCAACCCGACGTCAACCCGG
oAF1260	GTTGACTTCGGGATGCAGCTCGC
oAF1261	GCATCCCGAAGTCAACCCGGACGAGG
oAF1262	CGTCGGGTTGCAGCTCACGTGCC
oAF1263	GAGCTGCAACCCGACGTCAACCCCGAC
oAF1301	GTTCCGGTCAGGCTGCAGCTCGGCGGCCAG
oAF1302	GAGCTGCAGCCTGACCGGAACTCCGATC

References

1. Zolkiewski M, Kessel M, Ginsburg A, & Maurizi MR (1999) Nucleotide-dependent oligomerization of ClpB from Escherichia coli. *Protein Sci* 8(9):1899-1903.
2. Fay A & Glickman MS (2014) An essential nonredundant role for mycobacterial DnaK in native protein folding. *PLoS Genet* 10(7):e1004516.
3. Rath A, Glibowicka M, Nadeau VG, Chen G, & Deber CM (2009) Detergent binding explains anomalous SDS-PAGE migration of membrane proteins. *Proc Natl Acad Sci U S A* 106(6):1760-1765.
4. Snapper SB, Melton RE, Mustafa S, Kieser T, & Jacobs WR (1990) Isolation and characterization of efficient plasmid transformation mutants of Mycobacterium smegmatis. *Mol Microbiol* 4(11):1911-1919.
5. Muona M, Aranko AS, & Iwai H (2008) Segmental isotopic labelling of a multidomain protein by protein ligation by protein trans-splicing. *Chembiochem* 9(18):2958-2961.